



# Perturbation-enhanced feature correlation filter for robust iris recognition

M. Zhang Z. Sun T. Tan

Center for Biometrics and Security Research, National Laboratory of Pattern Recognition, Institute of Automation, Chinese Academy of Sciences, P.O. Box 2728, Beijing 100190, People's Republic of China  
 E-mail: znsun@nlpr.ia.ac.cn

**Abstract:** Visual pattern of human iris provides rich texture information for personal identification. However, it is challenging to match intra-class iris images with large variations in applications. This study proposes a perturbation-enhanced feature correlation filter (PFCF) for robust iris matching. PFCF is developed based on quad-phase minimum average correlation energy filter, but it has two significant improvements. First, PFCF is performed on Gabor filtered iris images to encode both local and global features. On the one hand, Gabor images can enhance the local details of iris texture. On the other hand, correlation filters describe the regional appearance information and measure the global similarity between iris images efficiently. Secondly, artificially perturbed iris images are generated to model intra-class variations. Also, a set of additional correlation filters are developed accordingly as the gallery templates. The decision is determined by the fusion result of multiple correlation filters. Therefore PFCF not only takes the advantages of Gabor images and correlation filters but also enlarges the amount of enrolled templates for robust iris matching. Extensive experiments on three challenging iris image databases demonstrate that the proposed method outperforms the state-of-the-art methods according to its robustness against deformation, rotation, occlusion, blurring and illumination changes in iris images.

## 1 Introduction

Iris is the frontal annular part of human eye and exhibits rich texture information under near infrared illumination. Iris texture is highly discriminating and stable during life. Besides, iris images can be captured at a distance in a non-invasive manner, thus iris recognition provides a promising method for personal identification [1].

The first successful iris recognition algorithm was proposed by Daugman [1], where odd and even Gabor filters were utilised for iris feature extraction. After filtering, an iris image was encoded to a sequence of binary iris codes. Finally, the dissimilarity between two iris images is determined by the Hamming distance (HD) between their iris codes. This classical method has been widely known and used in commercial applications. Since then, many researchers have devoted their minds to technical innovation of iris recognition and proposed a large number of iris recognition algorithms. Wildes *et al.* [2] used four-level Laplacian pyramid to represent iris patterns. Boles and Boashash [3] calculated wavelet zero-crossings features over concentric circles on the iris. Ma *et al.* [4] extracted position sequence of local sharp variation points as iris features after wavelet filtering. Sun and Tan [5] proposed qualitative representation of iris patterns using ordinal measures. Most of the state-of-the-art iris recognition methods mainly use local features to encode the fine details of iris texture.

Compared with local features mentioned above, correlation filters capture global variance information to describe the visual appearance of large regions. VanderLugt [6] pioneeringly introduced correlation filters into pattern recognition. Since then Kumar [7] did a lot of research work in this area. Some advanced filters were developed to achieve fast and accurate results in pattern recognition, for example, minimum average correlation energy (MACE) filters [8], quad-phase minimum average correlation energy (QP-MACE) filters [9], distance classifier correlation filters (DCCF) [10], optimal tradeoff circular harmonic function (OTCHF) [11], and so on. Kumar and co-workers [12–14] applied the advanced correlation filters to iris recognition and achieved encouraging results.

Iris features extracted from local image regions describe detailed information of iris texture. Most existing iris local features can be used in iris representation and matching efficiently and effectively. However, these methods are usually based on a point-to-point matching strategy, thus the matching results are easily affected by occlusions, misalignment, non-linear iris deformation, and so on. On the contrary, correlation filters mainly focus on global characteristics of iris patterns and represent the whole appearance properties of the iris images. They are less sensitive to photometric and geometric distortions. Therefore it is necessary to complement local features with global features to achieve the best possible recognition accuracy. Many researchers have done some work on fusion

of local and global iris features. Sun *et al.* [15] proposed a cascading fusion algorithm of local minutiae features and global blob patterns. Thornton [16] and Zhu *et al.* [17] fused local features and correlation filters for robust biometric recognition.

It is desirable to encode robust visual features for iris recognition but it is a challenging task. It is impossible to represent all possible intra-class variations in single iris template. An alternative way is to enlarge the amount of gallery images (or templates). The more gallery images (or templates) are used, the higher the probability to successfully match the probe iris images. It is a common practice in handwritten character recognition [18–20] that researchers usually use perturbed images to model distortion of characters to obtain sufficient training samples. The perturbation models cover large amount of writing habits to improve recognition accuracy.

In this paper, we propose perturbation-enhanced feature correlation filter (PFCF) for robust iris recognition. Gabor images are used to represent iris local features and correlation filters capture global information for measuring similarity of regional features. Meanwhile, perturbed original gallery images are generated to model intra-class variations of probe ones. In this paper, the perturbation method mainly aims to model deformed, blurred, misaligned iris images, which are typical challenging samples in real applications. With the help of the perturbation model, we generate a group of correlation filters for each class and combine the correlation results to achieve a better iris matching result.

More specifically, we address the problem of robust iris recognition and propose to recognise low-quality iris images based on cascaded correlation matching of perturbed Gabor images. As shown in Fig. 1, in the first stage, we use Gabor filters to extract Gabor images from gallery and probe iris images. Then a probe Gabor image is filtered by the correlation filter designed by the gallery Gabor images. If the correlation result is not in the defined range ( $[T_l, T_h]$ ), it outputs directly the matching score of the gallery and the probe images. Otherwise, the gallery images are taken into the next step for perturbation generation. In this step, we artificially generate several groups of perturbed iris images to design perturbed correlation filters and obtain a number of correlation results. At last, the combination of these correlation results is given as the matching score.

There are two main contributions of our work: (i) we apply global matching on local features to describe iris patterns and achieve a better result than either of them; (ii) we use perturbation generation to enlarge the amount of gallery images for further matching score fusion. Meanwhile, additional computational cost is limited due to the cascade

strategy. The proposed method is robust to noise, occlusion, blur, illumination changes and misalignment in extensive experiments.

The remainder of this paper is organised as follows: Section 2 introduces the motivation of our work. The technical details of the algorithm are described in Section 3. Section 4 provides the experimental results on three challenging iris image databases. Finally, Section 5 concludes the paper.

## 2 Motivation

In real applications, iris images captured from the same iris can appear very different. The difference is introduced due to many factors, for example, noise from the device, occlusions by eyelids and eyelashes, spectral reflections, defocus, motion blur, and so on. Plenty of iris recognition methods have emerged to solve these problems; however, no one is perfect. We can fuse complementary methods to make up their drawbacks to improve recognition performance.

Gabor filters have been widely used in biometrics such as iris recognition and face recognition. Two-dimensional (2-D) Gabor filters have some desirable characteristics [21]: (i) they are linear filters; (ii) they are all generated from one mother wavelet by dilation and rotation; (iii) they are Gaussian filters modulated by sinusoidal plane wave; and (iv) they refine the high frequency of images and focus on details of the image. In [21], Daugman also found that Gabor wavelet filters can model the simple cells in mammalian visual cortex. Thus, Gabor filters are particularly considered to be the appropriate ones to represent texture features and useful for texture discrimination. In recent years, Gabor features are used efficiently in image processing and biometrics. For instance, in the method proposed by Daugman [22], iris images are encoded into iris codes after Gabor wavelet filtering, which are effective to discriminate iris textures. However, Gabor features are point-to-point matched traditionally. The recognition results of this method are usually influenced by deformation, occlusion, and so on. The point-to-point matching method requires high quality of iris images, which is the bottleneck of the method.

QP-MACE filter [9] method synthesises a correlation filter  $h(i, j)$  from several registration iris images and builds a sharp peak in correlation plane when the test iris image  $x(i, j)$  is authentic. The correlation result  $R_{xh}(s, t) = \sum_{i=0}^M \sum_{j=0}^N x(i, j)h(i + s, j + t)$  indicates the similarity between  $x(i, j)$  and  $h(i, j)$ . The correlation operation can be seen as an integrative operation [23], because no single value from the image or the filter makes great influence on the correlation result. QP-MACE filter focuses on global iris features in a certain region, thus it is insensitive to

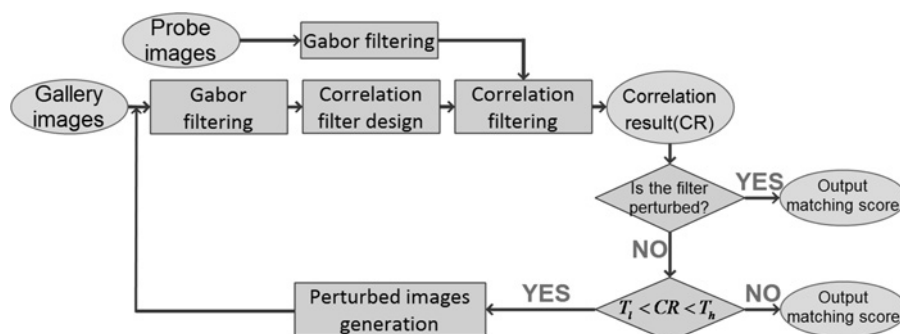


Fig. 1 Flowchart of the proposed iris recognition method based on PFCF

deformation, occlusion and in-built shift. Meanwhile, the filter suppresses the side lobes and sharpens the correlation peak in the correlation plane, thus it can enhance the distinction and discrimination of iris image classes. When the iris image quality is low, correlation measurement can achieve a better result than point-to-point matching. However, the drawback of correlation filter is that it is not robust to in-built noise. If there is much noise in the input images, the performance of correlation filters will decrease.

We find that QP-MACE filter can complement the drawback of point-to-point iris matching strategy. Meanwhile, Gabor images contain little in-built noise, thus they are more suitable as the input of QP-MACE filter than original iris images. For the complementarity of these two methods, fusion of them can describe iris images much comprehensively and improve system performance. The first motivation of our work is to use correlation matching of Gabor images to achieve a better recognition performance.

Although fusion of two sets of complementary features can achieve a better result, there are also much noisy factors decreasing recognition accuracy. Blurred, deformed, occluded, rotated iris images are typical samples degrading iris recognition performance. In general, we know that if there is more variety of templates for matching, the recognition performance will increase. However, we usually do not have sufficient amount of gallery images. Thus, the second motivation of our work is to artificially generate perturbed images to enlarge the amount of gallery iris images for robust iris recognition.

### 3 Technical details

#### 3.1 Framework of the proposed method

As shown in Fig. 1, we propose a novel method named PFCF for cascaded correlation matching of perturbed Gabor images. There are mainly four steps in the proposed method. At the very beginning, all normalised gallery and probe iris images are filtered by Gabor filters. The filtering results (namely Gabor images) are obtained and taken as the input data of the next stage. Then several gallery Gabor images are selected to design QP-MACE filters. In our experiments, a correlation filter is designed by three gallery Gabor images from the same class. Thirdly, a probe Gabor image is filtered by a designed filter. If the correlation result is not in the defined threshold region ( $[T_l, T_h]$ ), it is directly taken as the matching score of the class and the probe image. Otherwise, the gallery images are taken into the last stage for perturbation generation. In this stage, the probe image is filtered by the correlation filters which are designed by artificially generated perturbed iris images. Finally, the combination of correlation results is defined as the matching score of the class and the probe image.

#### 3.2 Gabor images

In recent years, Gabor filtering-based methods have been used widely in biometrics. Two-dimensional Gabor filter  $G(x, y)$  can be expressed by the following equation in the space domain [1]

$$\begin{aligned} G(x, y) &= e^u \times e^v \\ u &= -\pi[(x - x_0)^2/\alpha^2 + (y - y_0)^2/\beta^2] \\ v &= -2\pi i[u_0(x - x_0) + v_0(y - y_0)] \end{aligned} \quad (1)$$

where  $(x_0, y_0)$  is a certain position in the given image,  $(\alpha, \beta)$  controls the width and length of the filter and  $(u_0, v_0)$  is used for modulation.

The convolution results of iris images and Gabor filters are called Gabor images in this paper. In the correlation filtering stage, gallery Gabor images are used to design the correlation filters and probe Gabor images are filtered for identification.

#### 3.3 Feature correlation filter

After Gabor filtering, three gallery Gabor images  $y_1, y_2, y_3$ , which are extracted from gallery iris images  $x_1, x_2, x_3$ , from the same class are utilised to design the QP-MACE filter [9] of this class. The Gabor image  $y_p$  extracted from a probe iris image  $x_p$  is filtered by the designed filter. The correlation result is a matrix with the same size of  $y_p$ , and the matrix is also called correlation plane. After correlation calculation of the filter and the probe Gabor image, there are two possible outcomes. If there is a sharp peak in the correlation plane,  $x_p$  is accepted as genuine. Otherwise, it is considered as an imposter. The flowchart of Gabor correlation filter is shown in Fig. 2.

An iris image is denoted as  $x_i$  and its Gabor image as  $y_i$ . The feature extraction process can then be written as  $y_i = f(x_i)$ , where  $f$  means Gabor filter function. As is shown in Fig. 2, to obtain a high correction rate, the peak in the correlation plane must be sharpened and the side lobes must be suppressed [8]. One of the most efficient ways to solve this problem is to minimise the energy in the correlation plane. We take images  $x_i$  ( $i = 1, 2, 3$ ) to design QP-MACE filter  $h$  in the feature domain as the process shown in [9]. The correlation result of  $h$  and  $y_i$  in the feature domain is  $g_i = y_i \otimes h = f(x_i) \otimes h$ , where  $\otimes$  denotes correlation process. Let  $G_i, Y_i$  and  $H$  be the 2-D Fourier transform of  $g_i, y_i$  and  $h$ , respectively, and they all have the same size of  $m \times n$ . We take three images to design the filter as mentioned above, for  $G_i(p, q) = Y_i(p, q) H^*(p, q)$  and  $|H^*(p, q)|^2 |H(p, q)|^2$ , where  $H^*(p, q)$  means transpose  $H(p, q)$ , thus the average correlation energy (ACE) is [8]

$$\begin{aligned} \text{ACE} &= \frac{1}{3mn} \sum_i^3 \sum_p^m \sum_q^n |G_i(p, q)|^2 \\ &= \frac{1}{3mn} \sum_i^3 \sum_p^m \sum_q^n |Y_i(p, q)|^2 |H(p, q)|^2 \end{aligned} \quad (2)$$

We transform  $Y_i(p, q)$  into a diagonal matrix  $Z_i(p, q)$  whose diagonal elements are all from  $Y_i(p, q)$  and others are 0. When  $H$  is expressed as a vector  $\tilde{h}$ , the ACE becomes [8]

$$\begin{aligned} \text{ACE} &= \frac{1}{3mn} \sum_i^3 \sum_p^m \sum_q^n (\tilde{h}' Z_i) (Z_i^* \tilde{h}) \\ &= \tilde{h}' \left( \frac{1}{3mn} \sum_i^3 \sum_p^m \sum_q^n Z_i Z_i^* \right) \tilde{h} \\ &= \tilde{h}' D \tilde{h} \end{aligned} \quad (3)$$

where the superscripts  $'$  denotes conjugate transpose.

To minimise ACE, the side lobes of correlation output must be restricted. Let  $r$  stand for a restricting matrix to define the correlation result in  $(0, 0)$ . The restricting equation is as

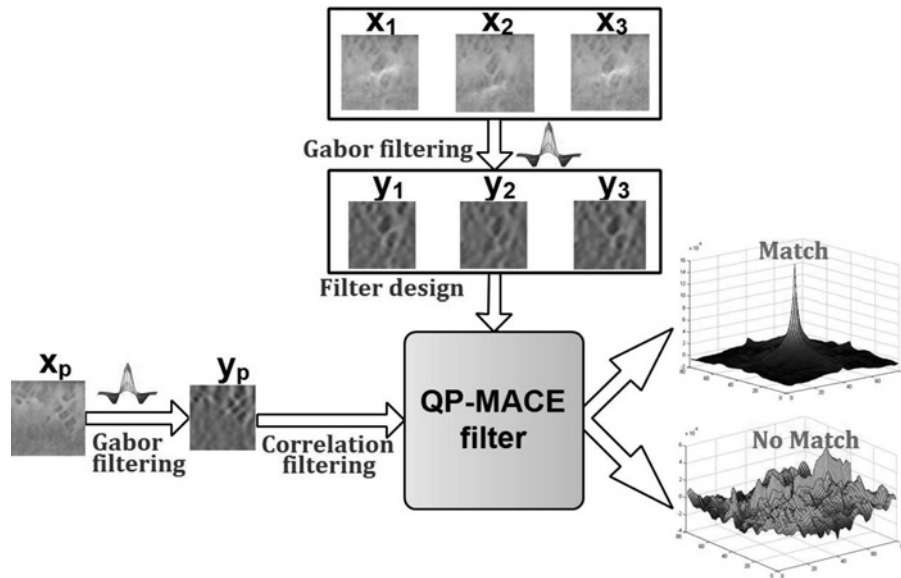


Fig. 2 Flowchart of feature correlation filter

follows [8]

$$W\tilde{h} = r \quad (4)$$

where columns of matrix  $W$  are vector Fourier representation of  $Y_i$ .

The filter minimises ACE in (3) subject to the constraints in (4). Thus [8]

$$\tilde{h} = D^{-1}W(W'D^{-1}W)^{-1}r \quad (5)$$

To describe phase information qualitatively, QP-MACE filter is formed as follows [9]

$$h_{QP-MACE}(u, v) = a + bi$$

$$a = \begin{cases} +1, & \text{if } R(\tilde{h}(u, v)) \geq 0 \\ -1, & \text{if } R(\tilde{h}(u, v)) < 0 \end{cases} \quad (6)$$

$$b = \begin{cases} +1, & \text{if } S(\tilde{h}(u, v)) \geq 0 \\ -1, & \text{if } S(\tilde{h}(u, v)) < 0 \end{cases}$$

where  $R(\tilde{h}(u, v))$  means the real part of  $\tilde{h}(u, v)$  and  $S(\tilde{h}(u, v))$  means the imaginary part of  $\tilde{h}(u, v)$ . This filter retains the qualitative phase information, and it only needs 2 bits for each point. It can not only save memory, but also greatly enhance calculation speed [9].

To characterise the sharpness of peak in the correlation plane, peak-to-side lobe ratio (PSR) is introduced. PSR is defined as [9]

$$PSR = \frac{p - \mu}{\sigma} \quad (7)$$

where  $p$  means the maximum value in the correlation plane,  $\mu$  and  $\sigma$  are the mean value and standard deviation in the correlation plane, respectively. PSR measures the difference between peak and side lobes instead of peak value. The sharper the peak is, the greater the PSR is. It can measure how well a given image matches the given filter.

### 3.4 Cascaded matching of perturbed iris images

In real applications, acquired iris images are usually affected by some external factors, such as noise, occlusion, deformation, and so on. A very simple idea to cope with such factors is to use a large amount of registration images. However, we usually cannot get enough images for registration. Inspired by [18–20], we introduce the idea of perturbation into our iris recognition framework. Our approach aims at representing the deviations of input iris images and modelling the variety of iris images, for example, deformed, blurred, misaligned images, and so on. We artificially generate iris images to design multiple correlation filters for each class.

Meanwhile, we use two-stage cascaded perturbed image matching to save computational time. At the first stage, original gallery iris images are taken to design filters. In this stage, perturbed images are not applied. Most iris images can be correctly recognised based on limited number of correlation filters. However, when the matching score is near to the decision boundary, the iris images cannot be confidently recognised as genuine or imposter samples, so the second stage is activated. We define two thresholds  $t_l$  and  $t_h$ , where  $t_l < t_h$ . If the correlation result is greater than  $t_l$  and less than  $t_h$ , we put the gallery and probe images into the second stage. In this stage, we use the original gallery images to artificially generate perturbed images with different parameters.

How we generate perturbed images is as follows and some perturbed normalised iris image examples are shown in Fig. 3.

1. Deformed images: let  $f(x, y)$  be an original normalised iris image and  $g(u, v)$  is the artificially deformed one. We linearly scale the  $y$ -coordinate to the interval  $[0, 1]$  and mark the new coordinate as  $t$ . So we set [20]

$$\begin{cases} u = x \\ v = \omega(a, t) \end{cases} \quad (8)$$

where  $a$  is a non-zero constant. Meanwhile, in (8), the

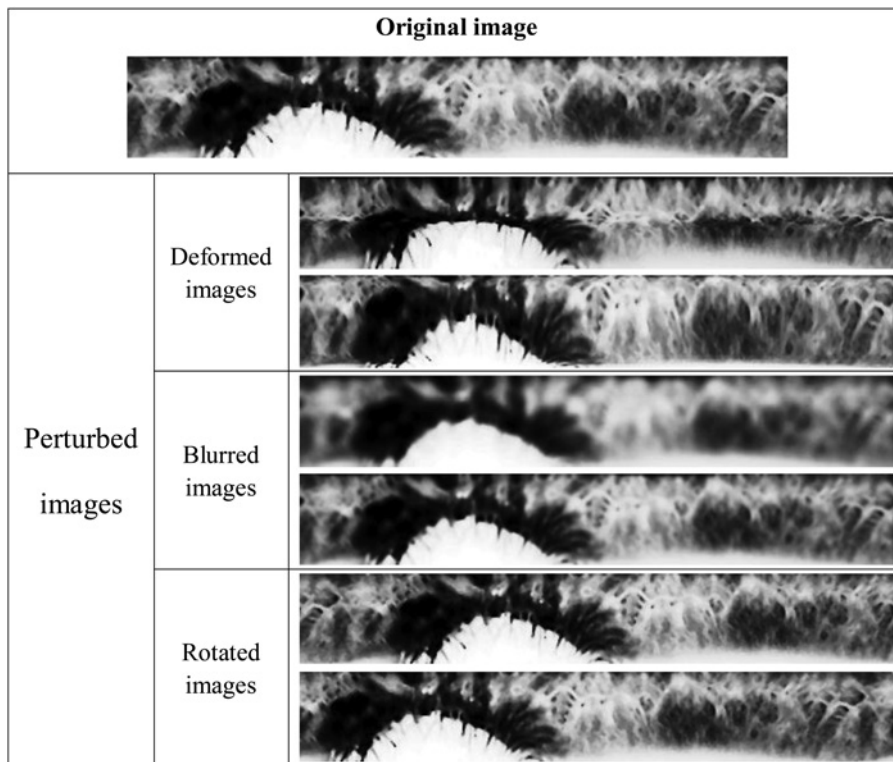


Fig. 3 Perturbed normalised iris images

warping function is [20]

$$\omega(a, t) = \begin{cases} 0.5 \times \frac{1 - e^{-2at}}{1 - e^{-a}}, & 0 \leq t \leq 0.5 \\ 0.5 + 0.5 \times \frac{1 - e^{2a(t-0.5)}}{1 - e^a}, & 0.5 < t \leq 1 \end{cases} \quad (9)$$

In our experiments,  $a$  varies from  $-0.3$  to  $0.3$ .

2. Blurred images: we use circular averaging filter to generate blurred images. The radius of circular averaging filter varies from 1 to 5 in the experiments.

3. Rotated images: we rotate the normalised iris images to left or right by several pixels (less than 20 pixels) to generate many rotated images for misaligned image matching.

As shown in Fig. 4,  $I_1, I_2$  and  $I_3$  are taken from the same class to design the correlation filter of this class. In our experiments, we artificially deform, blur and rotate images step by step and we mark the images in each step as  $DI_i (i = 1, 2, 3)$ ,  $BI_i (i = 1, 2, 3)$  and  $RI_i (i = 1, 2, 3)$ , respectively, where each step adds another operation cumulatively. At last, we design a correlation filter based on the three-step perturbed images  $RI_i (i = 1, 2, 3)$ . In each step, we define many groups of parameters to generate perturbed images, and thus we can obtain a lot of feature correlation filters for a certain class. For example, in a certain class, we define  $m, n, k$  groups of parameters in

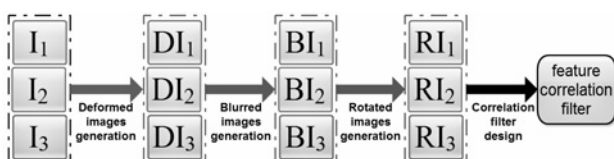


Fig. 4 Perturbed correlation filter design

deformation step, blurring step and rotation step, respectively, and the three images are perturbed with the same group of parameters in each step,  $m \times n \times k$  perturbed feature correlation filters can be designed for this class.

After perturbed feature correlation filter design, we obtain a filter group containing  $m \times n \times k + 1$  feature correlation filters (1 original and  $m \times n \times k$  perturbed filters) for each class. Thus, for a test iris image, we can obtain  $m \times n \times k + 1$  correlation results  $CR_i = \text{img} \otimes CF_i (i = 0, 1, \dots, m \times n \times k)$ , where  $\text{img}$  means the test iris image and  $CF_0$  means the original feature correlation filter. Finally,  $\max(CR_i)$  is designed as the matching score of the test image and the registration class.

## 4 Experiments

### 4.1 Databases

To evaluate the proposed method, three iris image databases are used in our experiments. They are CASIA-Iris-Lamp [24], CASIA-Iris-Thousand [25] and ICE 2005 databases [26]. Some challenging examples from these databases are shown in Fig. 5.

The first one is CASIA-Iris-Lamp Database [24], which will be abbreviated as ‘Lamp’ in the following. When the iris images were acquired, a lamp was turned off/on to lead to pupil dilation and contraction. The ratio of pupil radius to iris radius varies from 0.19 to 0.67 in this database. Large intra-difference is introduced to the database due to elastic deformation of iris. In this database, there are more than 800 classes and each class contains about 20 images.

The second one is CASIA-Iris-Thousand [25], which will be abbreviated as ‘Thousand’ in the following. This database contains 20 000 iris images from 1000 persons. It is the first public iris database containing 1000 subjects,

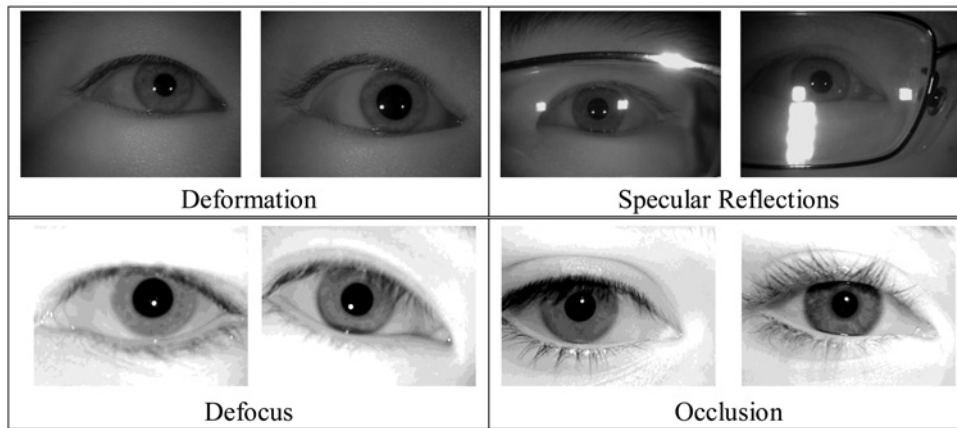


Fig. 5 Some challenging examples from iris image databases

thus it is very suitable for the research of iris feature representation and the evaluation of iris recognition algorithms. The iris images in this database were acquired under various environmental lights in only one session. The main source of intra-class variation is iris elastic deformation, occlusion and specular reflections.

The third one is ICE 2005 Iris database [26], which will be abbreviated as 'ICE' in the following. There are 2953 images from 132 subjects in the database, which was released by the National Institute of Standards and Technology (NIST). This database contains large amount of low-quality iris images, for example, defocus, occlusions by eyelashes and eyelids, deformation, and so on.

#### 4.2 Experimental results

To illustrate the effectiveness of the method proposed in this paper, we compare it with other three state-of-the-art iris recognition algorithms on the three challenging databases. In each compared algorithm, there are also three linear normalised iris images selected randomly from each class for registration and some of the rest images (more than 4 and less than 12 images) are taken for test. The first compared algorithm is Gabor wavelet filtering with classification with HD [1]. Iris images are filtered by Gabor filters at different scales and positions, and the phase information of filtering results is encoded as iris codes. The similarity of two images is defined as the HD between their iris codes. The second one is QP-MACE filter [9] in space domain. The similarity between a probe image and a filter is measured by PSR. The last one is ordinal measures [5]. Tri-lobe ordinal filters are used to represent iris features qualitatively. HD between ordinal codes is used to determine the dissimilarity of two iris images.

In the proposed algorithm, gallery and probe iris images are filtered by multi-orientation Gabor filters to extract Gabor images. In correlation filter design stage, each gallery Gabor

image is divided into several patches with overlap and there is a filter designed in each patch position. The probe one is also divided into the same number and size of patches. Each patch of probe Gabor images is filtered by the filter in the corresponding location. In the experiment, small image patch cannot contain enough global information. It also consumes too much computational cost, because time cost of patch filter designing and filtering with different sizes is similar, and the total computational cost will increase with the growth of the number of patches. However, if the patch size is too large, some negative factors will be introduced, such as deformation and occlusion. To achieve the trade-off between computational cost and algorithm robustness, the size of patches is selected as  $32 \times 32$  and there is  $16 \times 32$  or  $32 \times 16$  overlap between each neighbour patch pair. Two performance indicators, equal error rate (EER) and discriminating index [1] (DI) are used to evaluate the performance of the proposed and compared methods.

As shown in the proposed framework in Fig. 1, we used cascaded flowchart to save computation time. In the perturbation generation stage, we used three perturbation models, deformation, blurring and rotation. In the experiments, we choose six groups of deformation parameters, four groups of blurring parameters and six groups of rotation parameters, thus we can obtain 144 ( $6 \times 4 \times 6$ ) perturbed correlation filters for a certain class. After correlation filtering, matching score is the max one of all the correlation results.

Recognition results, including EER and DI, on three databases are shown in Table 1. Besides, the entire ROC curves on these databases are shown in Figs. 6–8, respectively. The experimental results on three challenging databases are shown above. As shown in Fig. 9, to illustrate the effectiveness of our method more directly, we take an example of perturbed correlation filtering.  $I_1$ ,  $I_2$ ,  $I_3$  and  $img$  are all the original normalised iris images from the same class.  $I_1$ ,  $I_2$ ,  $I_3$  are taken to design a correlation filter, and

Table 1 Experimental results on three iris image databases

	Lamp		Thousand		ICE	
	EER, %	DI	EER, %	DI	EER, %	DI
Gabor filtering	3.47	2.1319	4.10	3.0173	3.78	3.1133
QP-MACE	3.14	3.5159	4.52	3.1380	1.95	3.4738
ordinal measures	1.22	4.1829	0.43	4.2622	0.61	4.5908
PCFC	0.37	4.0133	0.40	3.4658	0.24	3.7452

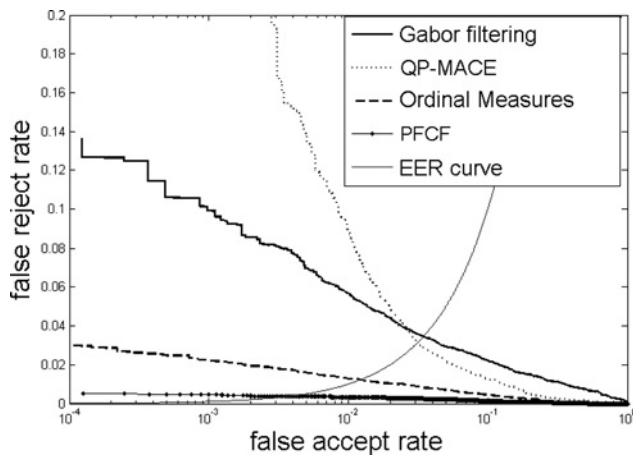


Fig. 6 ROC curves on the Lamp database [24]

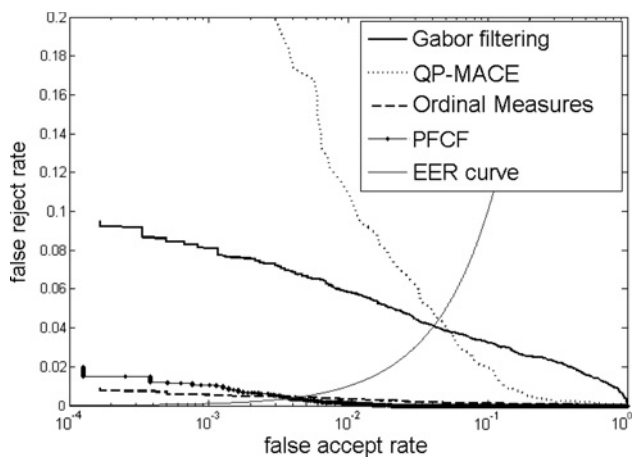


Fig. 7 ROC curves on the Thousand database [25]

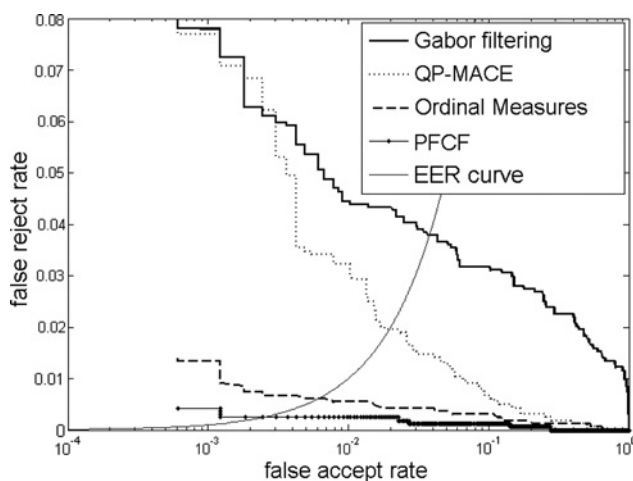


Fig. 8 ROC curves on the ICE database [26]

the correlation result (matching score) of *img* and the filter is 5.84. However, after perturbation, several groups of perturbed images based on  $I_1, I_2, I_3$  are generated and they are taken to design perturbed correlation filters. The matching score of *img* and the perturbed correlation filters is 9.62, which is improved significantly.

Compared to other methods, PFCF achieves better results. On the one hand, the QP-MACE filters of Gabor images fuse

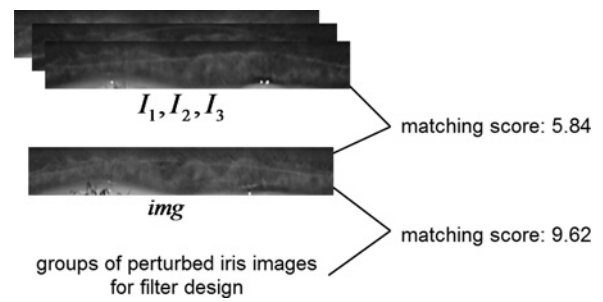
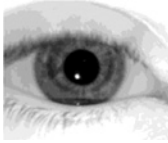

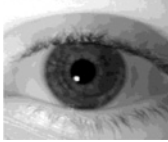
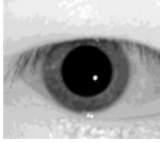



Fig. 9 Example of PFCF result

Gabor images and traditional correlation filters efficiently. In Gabor filtering stage, the intra-class iris image details are enhanced and intra-difference noise is filtered out. The extracted Gabor images are robust to illumination changes and noise, thus the Gabor images are more stable than the original images and suitable to be the input of correlation filters. Different from Gabor filtering, the proposed algorithm measures the similarity between Gabor images by correlation results. In correlation process, sharpened peak and suppressed side lobes can increase the distribution difference between intra-class and inter-class iris samples.

Table 2 Some challenging examples in the experiments

	Gabor filtering	QP-MACE	Ordinal measures	PFCF
 occluded	×	✓	✓	✓
 rotated	✓	×	✓	✓
 blurred	×	×	×	✓
 deformed & occluded	×	×	×	✓
 deformed	×	×	×	✓

Meanwhile, the proposed method describes iris pattern comprehensively and it is insensitive to occlusion and misalignment. On the other hand, we introduced perturbed images to design more correlation filters. The artificially generated iris images model the deviation of acquired iris images efficiently and effectively. With the help of perturbation model, the amount of gallery images is enlarged and the recognition performance is improved.

In Table 2, there are several challenging iris image examples utilised in the experiments. Some external factors make influence on the quality of the iris images, and the example iris images are deformed, blurred, rotated or occluded by eyelash and eyelids. Deformation caused by illumination change makes bad influence on recognition accuracy. Eyeglasses usually produce specular reflection and make texture of iris images blurred. Head motion usually leads to iris image blur and rotation. These example images cannot be well addressed by other algorithms. However, in the experiments the proposed method classifies them correctly. Iris texture details distributed in certain scale and orientation are enhanced and intra-difference image components are suppressed in the Gabor filtering stage. Then correlation filters preserve global information and produce large discrimination of iris classes. At last, the cascaded perturbation generation strategy enlarges the amount of gallery images efficiently for further robust matching. Especially, it is shown in the experiments that the PFCF method achieves a most encouraging result in the Lamp database. Although we deformed original images very roughly in the experiments, the generated images benefit robust matching rather than introduce intra-difference into the system due to the integrative operation of correlation filters and combination of multiple correlation results. Thus, the recognition accuracy in the Lamp database is much better than other algorithms. Compared with other algorithms, the proposed iris recognition method is more robust.

## 5 Conclusions

Iris recognition is promising for identity authentication due to the richness of iris texture information. Although an iris pattern is naturally an ideal identifier, the development of high-performance iris recognition algorithm is still a challenging task. Automatic iris recognition has to face unpredictable variations of iris images in real-world applications.

To improve recognition accuracy in some challenging situations, a novel method namely PFCF is proposed in this paper. One key point of our method is that we used correlation filters of Gabor images for robust correlation matching of iris images in Gabor feature domain. It combines the advantages of Gabor images and correlation filters to reserve local and global features efficiently for robust iris recognition. In correlation matching of Gabor images stage, Gabor filters can enhance iris texture details distributed in certain scale and orientation and suppress intra-difference image components distributed in other texture spectrum channels, such as additive noise. The extracted Gabor images are also robust against illumination changes, thus the Gabor images are more stable than original iris images as input data of correlation filters. Meanwhile, the correlation filters are utilised for Gabor images matching instead of HD measurement. Compared with traditional HD measurement, this method can produce higher intra-class and inter-class discrimination with the help of the sharp peak in the correlation plane. This method encodes both local and global iris features for reliable identity verification.

The other key point of the proposed method is that some artificially generated iris images are introduced into the recognition framework for further matching. This idea is a novel solution compared with common robust iris matching methods. The perturbation method models variety of acquired iris images instead of restoring low-quality images. The perturbation method is more effective and easy to enlarge the amount of gallery images for further matching. Meanwhile, because of integrative operation of correlation filters and the combination strategy of multiple correlation results, the perturbation model improves robustness of iris recognition system instead of introducing noise into the system.

We set up some experiments on three challenging iris image databases to evaluate the performance of the proposed algorithm. It is shown that the proposed method can perform better than the other state-of-the-art iris recognition algorithms. PFCF method achieves encouraging results and indicates a successful way to improve the state-of-the-art iris recognition performance by combination of local and global features. Besides, the efficient perturbation generation method applied in PFCF method models variety of iris images for further matching and result combination efficiently. Owing to the characteristics mentioned above, the proposed method is robust to noise, occlusion, blur, illumination changes and misalignment.

In the future, our work will focus on improving iris recognition performance by optimisation of the components in the PFCF method. For example, Gabor images can be replaced by other robust local iris features, for instance, ordinal features. Correlation filters also can be replaced by other advanced filters, such as DCCF, OTCHF, and so on. Meanwhile, we can see that the perturbation method improves the recognition rates efficiently and effectively. However, the perturbation generation model will be improved for more accurate matching. The variants of the proposed method may achieve a better result in the future.

## 6 Acknowledgments

This work is funded by National Natural Science Foundation of China (grant no 61075024) and International S&T Cooperation Program of China (grant no. 2010DFB14110).

## 7 References

- 1 Daugman, J.G.: 'High confidence visual recognition of persons by a test of statistical independence', *IEEE Trans. Patt. Anal. Mach. Intell.*, 1993, **15**, (11), pp. 1148–1161
- 2 Wildes, R.P., Asmuth, J.C., Green, G.L., *et al.*: 'A machine-vision system for iris recognition', *Mach. Vis. Appl.*, 1996, **9**, (1), pp. 1–8
- 3 Boles, W.W., Boashash, B.: 'A human identification technique using images of the iris and wavelet transform', *IEEE Trans. Signal Process.*, 1998, **46**, (4), pp. 1185–1188
- 4 Ma, L., Tan, T., Wang, Y., Zhang, D.: 'Local intensity variation analysis for iris recognition', *Patt. Recogn.*, 2004, **37**, (6), pp. 1287–1298
- 5 Sun, Z., Tan, T.: 'Ordinal measures for iris recognition', *IEEE Trans. Patt. Anal. Mach. Intell.*, 2009, **31**, (12), pp. 2211–2226
- 6 VanderLugt, A.: 'Signal detection by complex spatial filtering', *IEEE Trans. Inf. Theory*, 1964, **10**, pp. 139–145
- 7 Kumar, B.V.K.: 'Tutorial survey of composite filter designs for optical correlators', *Appl. Opt.*, 1992, **31**, (23), pp. 4773–4801
- 8 Mahalanobis, A., Kumar, B.V.K., Casasent, D.: 'Minimum average correlation energy filters', *Appl. Opt.*, 1987, **26**, (17), pp. 3633–3640
- 9 Savvides, M., Kumar, B.V.K.: 'Quad phase minimum average correlation energy filters for reduced memory illumination tolerant face authentication', in Josef Kittler, Mark S. Nixon (Eds.): 'Audio- and video-based biometric person authentication' (Springer, 2003), pp. 1056–1056



- 10 Mahalanobis, A., Carlson, D.W., Kumar, B.V., Sims, S.R.F.: 'Distance classifier correlation filters'. Proc. Society of Photo-Optical Instrumentation Engineers (SPIE), Bellingham, 1994, vol. 2238, pp. 2–13
- 11 Vijaya Kumar, B.V.K., Mahalanobis, A., Takessian, A.: 'Optimal tradeoff circular harmonic function correlation filter methods providing controlled in-plane rotation response', *IEEE Trans. Image Process.*, 2000, **9**, (6), pp. 1025–1034
- 12 Vijaya Kumar, B.V.K., Xie, C., Thornton, J.: 'Iris verification using correlation filters', in Josef Kittler, Mark S. Nixon (Eds.): 'Audio- and video-based biometric person authentication' (Springer, 2003), pp. 697–705
- 13 Thornton, J., Savvides, M., Vijaya Kumar, B.: 'Robust iris recognition using advanced correlation techniques', *Image Anal. Recogn.*, 2005, **3656**, pp. 1098–1105
- 14 Thornton, J., Savvides, M., Kumar, B.: 'Improved iris recognition using probabilistic information from correlation filters', *Adv. Biom.*, 2008, **2**, pp. 265–285
- 15 Sun, Z., Wang, Y., Tan, T., Cui, J.: 'Improving iris recognition accuracy via cascaded classifiers', *IEEE Trans. Syst. Man Cybern., Part C: Appl. Rev.*, 2008, **35**, (3), pp. 435–441
- 16 Thornton, J.: 'Matching deformed and occluded iris patterns: a probabilistic model based on discriminative cues'. PhD thesis, Carnegie Mellon University, 2007
- 17 Zhu, X., Liao, S., Lei, Z., Liu, R., Li, S.: 'Feature correlation filter for face recognition', *Adv. Biom.*, 2007, **4642**, pp. 77–86
- 18 Ha, T.M., Bunke, H.: 'Off-line, handwritten numeral recognition by perturbation method', *IEEE Trans. Patt. Anal. Mach. Intell.*, 1997, **19**, (5), pp. 535–539
- 19 Dahmen, J., Keysers, D., Ney, H.: 'Combined classification of handwritten digits using the virtual test sample method', in Josef Kittler, Fabio Roli (Eds.): 'Multiple classifier systems' (Springer, 2001), pp. 109–118
- 20 Leung, K.C., Leung, C.H.: 'Recognition of handwritten Chinese characters by combining regularization, Fisher's discriminant and distorted sample generation'. Proc. Int. Conf. Document Analysis and Recognition, Catalonia, Spain, July 2009, pp. 1026–1030
- 21 Daugman, J.G.: 'Uncertainty relation for resolution in space, spatial frequency, and orientation optimized by two-dimensional visual cortical filters', *Opt. Soc. Am. J.: Opt. Image Sci.*, 1985, **2**, pp. 1160–1169
- 22 Daugman, J.G.: 'How iris recognition works', *IEEE Trans. Circuits Syst. Video Technol.*, 2004, **14**, (1), pp. 21–30
- 23 Kumar, B.V.K.V., Mahalanobis, A., Juday, R.D.: 'Correlation pattern recognition' (Cambridge University Press, 2005)
- 24 CASIA-Iris-Lamp Database: <http://biometrics.idealtest.org/>
- 25 CASIA-Iris-Thousand Database: <http://biometrics.idealtest.org/>
- 26 ICE 2005 Iris Database: <http://www.nist.gov/itl/iad/ig/iris.cfm>